Office of the Chief Scientist for Human Factors

Human Factors Vertical Flight

Program Review
FY03

Dr. William K. Krebs, Vertical Flight Human Factors Program Manager

Federal Aviation Administration
AAR-100 (Room 907A)
800 Independence Avenue, S.W.
Washington, D.C. 20591
phone (202) 267-8758
e-mail: william.krebs@faa.gov
http://www.hf.faa.gov/krebs

The Federal Aviation Administration Office of the Chief Scientific and Technical Advisor for Human Factors (AAR-100) vertical flight human factors program is a relative new research domain. Research in this area is meant to identify specific human factors associated with helicopter flight regimes within the National Airspace System. Such issues include certification and regulation of civilian flights with night-vision-goggles devices, simultaneous non-interfering operations, and implications of tilt-rotor controls.

The following report summarizes projects between October 1st, 2002 and December 31st, 2003. These projects attempt to address requirements identified by the Federal Aviation Administration Flight Standards and Certification offices. The intent of this report is to allow Federal Aviation Administration sponsors to determine whether their requirements have been satisfactorily addressed, allow investigators to receive feedback from Federal Aviation Administration sponsors and other interested parties, and to provide feedback to the AAR-100 vertical flight human factors program manager on the quality of the research program. Basically, this document is a means of holding each group (sponsor, investigator, AAR-100 program manager) accountable to ensure that the program is successful.

The vertical flight human factors program research has focused on two areas: night vision goggles and simultaneous non-interfering operations. The requirements that are mapped to these projects are located in Appendix II.

The FY03 funded projects had $150,000 contract dollars and the proposed FY04 and FY05 projects will have an estimated $150,000 contract dollars each fiscal year.

To view project summaries, 3-23
To view requirements, 24-29

Address questions or comments to:

William K. Krebs, Ph.D.

Appendix I

Human Factors Vertical Flight

FY03 Project Summaries

NIGHT VISION IMAGING SYSTEM LIGHTING COMPATIBILITY ASSESSMENT METHODOLOGY

[*]H. Lee Task, Ph.D., [§]Alan R. Pinkus, Ph.D., [†]Maryann H. Barbato, [†]Martha A. Hausmann
[*]Task Consulting, Dayton, Ohio
[§]Air Force Research Laboratory, Wright-Patterson AFB, Ohio
[†]Sytronics, Inc., Dayton, Ohio

Aircraft cockpit lighting can interfere with the proper operation of night vision goggles (NVGs). Methods to verify compatibility between cockpit lighting and NVGs involve expensive equipment. An inexpensive alternative method to assess compatibility, that provides the same quality of results, is needed. Since the quality of the existing lighting compatibility methods has not been studied, it was necessary to determine the quality of existing methods and compare them to alternative methods using a night lighting simulator. The visual acuity-based evaluation method is relatively imprecise, but it can be implemented using alternative, inexpensive equipment and techniques. An alternative evaluation method, that makes use of the light output of the NVGs, looks promising. It provides a more precise acceptance/rejection criteria than the visual acuity method.

INTRODUCTION

Night vision goggles (NVGs) amplify and convert available ambient light at night to produce an image viewable by the observer that is hundreds or thousands of times brighter than the same scene viewed with the naked eye (see Fig. 1). Current NVGs used for flight are sensitive to wavelengths from about 625 nm or 665 nm (depending on objective lens coating) to about 900 nm. Unfortunately, most unmodified aircraft cockpit lighting emits considerable energy in this wavelength range that can make it very difficult or impossible to see through the windscreen with the NVGs.

Figure 1. F4949 night vision goggles

Unmodified aircraft cockpit lighting can interfere with the proper operation of NVGs in several specific ways. For each interference mechanism, the effect on the image seen through the NVGs is a reduction of the light level or contrast of the view outside the aircraft. This reduction in light level or contrast can be manifested as a reduction in visual acuity and/or as an observed loss of contrast or brightness. Many techniques have been developed to produce cockpit lighting, including instrumentation and displays, that are reasonably compatible with the operation of NVGs[1]. *Reasonably compatible* means there is sufficient light for the pilot to view his/her instruments and displays (note, pilots look under the NVGs to directly view their instruments) but the lighting is such that it does not significantly interfere with the image of the exterior scene viewed through the NVGs.

The US Air Force, Army, and Navy have pursued the use of NVGs for piloting aircraft for over 20 years. One of the first major issues to be addressed was cockpit lighting compatibility with the NVGs.[2] The military eventually developed a criteria that could be relatively easily, but not inexpensively, implemented to determine whether or not the cockpit lighting was night vision imaging system (NVIS) compatible. These criteria have been expanded considerably from their original concept and are documented in various publications[1,3,4,5,6,7]. The original basic concept was that no lighting source in the cockpit, when adjusted to the specified luminance level, should appear brighter through the NVGs than tree bark illuminated with natural clear starlight[7]. This concept was converted to photometric and radiometric criteria for various cockpit lighting sources. For example, electronic displays adjusted to produce an output luminance of 0.5 foot-Lamberts should not exhibit an NVIS radiance greater than 1.7 x 10^{-10} watts/cm^2-sr. The NVIS radiance is the radiance of the display as weighted by the spectral sensitivity curve of the NVGs. There are currently two published spectral sensitivity curves for NVGs used in flight, designated NVIS A and NVIS B. NVIS A spectral sensitivity starts at about 625 nm and NVIS B sensitivity starts at about 665 nm.

Although this approach provides easy to understand criteria for passing or failing a lighting system for NVIS compatibility, it also requires the use of expensive equipment to accurately measure the luminance and NVIS radiance values of the various light sources. Since this equipment is not conducive to a field assessment of NVIS compatibility, there is

a secondary approach that is used, based on visual acuity, that is described in the various military publications.[3] In this secondary approach, a trained evaluator sits in the cockpit of the aircraft while it is located in a dark, light-controlled hangar. A visual acuity chart (e.g., USAF 1951 Tri-bar Resolution Chart) is positioned 20 feet from the objective lens of the NVGs and illuminated to an NVIS radiance of 1.7 x 10^{-10} watts/cm^2-sr (tree bark in clear starlight). The cockpit lighting level is adjusted to an *operational level* so that it is easily visible to the evaluator. The evaluator then determines his/her visual acuity with the cockpit lighting system on and off. If there is any decrement in visual acuity between the on and off conditions, then the lighting system is considered unacceptable. If there are any reflections noted in the aircraft windscreen, then the visual acuity chart is to be repositioned, if possible, so that the evaluator is viewing directly through the reflection.

There has been essentially no research to determine the repeatability and/or reproducibility of either the NVIS radiance measurement method or the visual acuity assessment method of determining NVIS lighting compatibility. The primary objective of the research described herein was to develop an inexpensive NVIS lighting methodology that would produce essentially the same or better results than the documented military assessment techniques[8]. Particular emphasis was placed on the visual acuity approach, since it is the most often used method for performing a field assessment of cockpit lighting. It was therefore necessary to assess how good the currently used visual acuity method is and what other possible methods could be used to achieve equivalent or better results.

APPROACH

In order to develop an alternative method for the visual acuity-based approach, it was necessary to identify the specific elements of the method and produce inexpensive alternatives. The specific elements identified for devising alternatives were: 1) the visual acuity chart, 2) the calibrated illuminator, 3) a means of verifying the chart radiance, and 4) a means of determining that the test facility is sufficiently dark to conduct the test.

Several alternative methods to the visual acuity-based method were discussed and documented. One of these was selected for inclusion in the study.

In order to evaluate different NVIS compatible lighting assessment methodologies, it was necessary to devise a night lighting simulator (NLS) so that numerous assessments could be conducted under various controlled conditions.

VISUAL ACUITY METHOD ELEMENTS

Visual Acuity Chart: The baseline military method[6] uses a commercially available USAF 1951 Tri-bar resolution chart (medium or high contrast) that costs approximately $600. The alternative method chosen uses a PDF file of the USAF 1951 Tri-bar resolution chart that was located on the World Wide Web. The chart was laser printed on 8.5 x 11-inch white bond paper and mounted to a foam core back. Photometric and radiometric measurements of the alternative chart verified that it was comparable to the commercially available chart.

Illumination Source: The baseline military method uses a commercially available, calibrated illumination source that costs approximately $5000. The alternative method uses an inexpensive goose-neck lamp. A baffle with a 1/8 inch diameter hole covers the open end of the lamp housing. When the 7.5-watt light bulb is powered by 115 VAC, it provides approximately the correct irradiance at 20 feet. To correct for variability in line voltage and lumen output differences among light bulbs, an inexpensive ($150) illuminance meter was used. An empirically derived look-up table was used to adjust the chart-to-illuminator distance, in order to achieve the correct NVIS irradiance.

Verification of Illumination Level: The baseline military method makes use of two different NVIS radiance measurement devices (approximately $20,000 and $28,000) to verify the NVIS radiance of the white background of the chart. The alternative method verifies the light level by making use of the illumination meter, noted above, and the look-up table.

Test Facility Light Level: The baseline military method makes use of the NVIS radiance measurement equipment to verify that the facility is dark enough to conduct the test. The alternative method is to use the inexpensive visual acuity chart and verify that the evaluator, when looking through the NVGs, cannot resolve the largest pattern on the chart (20/90.3 Snellen acuity).

EVALUATION COMPARISON STUDY

Introduction: Although there are several mechanisms by which cockpit lighting can affect the NVGs, only two basic conditions were selected to be studied. These two conditions were: 1) a uniform light source (display) reflecting in the windscreen, and 2) a uniform display that is blocked by a glare shield from reflecting in the windscreen but may still be within the NVG field of view. The NLS was designed to produce these two conditions and provide a selectable level of NVIS radiance compared to

visible luminance. Using the NLS, three different assessment approaches were studied: 1) visual acuity decrement, 2) direct radiance measurement, and 3) NVG luminance output level measurement.

Observers: Six males and four females ranging in age from 23-51 participated in this study. Prior to participation in the study, all observers underwent a visual examination to insure they had normal or corrected acuity of 20/20 or better.

Apparatus: The lighting simulator (see Fig. 2) was positioned directly in front of the observer. The visual acuity chart was positioned 20 feet from the objective lens of the NVGs and illuminated with an incandescent lamp. The NVIS radiance on the chart was monitored using a Photo Research 1530AR radiometer. Model F4949C NVGs were used in this study. A Hoffman Engineering NVG 103 radiometer was used by the observers to measure the NVIS radiance of the interfering light source. The actual radiance and luminance of the lighting simulator was measured using an Instrument Systems Model 320 spectral scanning radiometer.

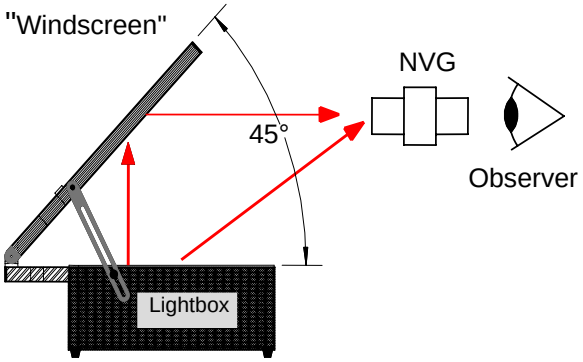

Figure 2. NLS in Reflective Mode

Procedure: Observers were seated behind the NLS and the armrest and seat height were adjusted. Since the NVGs were hand held, the armrest was positioned to allow proper alignment with the stimulus and to reduce fatigue. The room lights were turned off and the observer dark-adapted for 12 minutes. If the session involved the use of NVGs, observers were asked to focus them according to the procedure taught to them during their orientation. Prior to each task, the observer received a sufficient number of practice trials for familiarization with the task and equipment. For the reflected and non-reflected conditions, the following three tasks were counterbalanced. The NVIS radiance light levels were randomly presented for each task.

Task 1: Observers looked through a pair of F4949C NVGs at a USAF 1951 Tri-bar chart. A Photo Research 1530AR was used to monitor the NVIS radiance of the target. The observers identified the group and element number of the smallest pairs of horizontal and vertical bars they could resolve. They closed their eyes between each trial while the experimenter adjusted the NVIS radiance of the NLS. The experimenter instructed the observers to open their eyes and begin the next trial. Five data points were collected per NVIS radiance light level, for a total of 35 data trials for each of the reflective and non-reflective lighting conditions.

Task 2: The observers rested their elbows on the armrest while holding the Hoffman NVG 103. After focusing it, the observer aimed the device so it was perpendicular to the center of the NLS. They adjusted the brightness of the internal test patch located inside the Hoffman NVG 103 to match the brightness of the NLS. Once they were satisfied with their setting, the observers read the digital output on the NVG 103 and the experimenter recorded the data. Ten data points were collected per NVIS radiance level, for a total of 70 data trials for each of the reflective and non-reflective lighting conditions.

Task 3: The observers rested their elbows on the armrest and focused the right ocular of the NVGs. The experimenter attached an Extech Light ProbeMeter to the eyepiece of the right ocular with black masking tape. The observers held the goggles steady while aiming them through the simulated windscreen at the Tri-bar target. When the NVGs were steady, the observer signaled the experimenter, who then recorded the measurement (lux) from the digital readout of the light meter. The experimenter then adjusted the light level of the NLS and indicated when the next trial was to begin. This procedure was repeated ten times per light level for a total of 70 data trials for each of the reflected and non-reflected lighting conditions.

Results: Figure 3 is a summary of the raw data from one of the ten observers. The two columns correspond to the reflected and non-reflected conditions, respectively, and the three rows correspond to the visual acuity assessment (Task 1), NVIS radiance measurement using the NVG 103 (Task 2), and the NVG output luminance measurement (Task 3), respectively. For each observer, these raw data were converted to acceptance/rejection results and then combined. The visual acuity data were converted to an acceptance/rejection decision by comparing each of the individual's visual acuity data points for both the *off* and *on* cockpit lighting conditions. If the observer's visual acuity was worse for any given *on* condition than for the *off* condition, then that pair of points was scored as a *reject*. If the two acuities were the same or if the *on* condition was actually better

than the *off* condition, then it was scored as an *accept*.

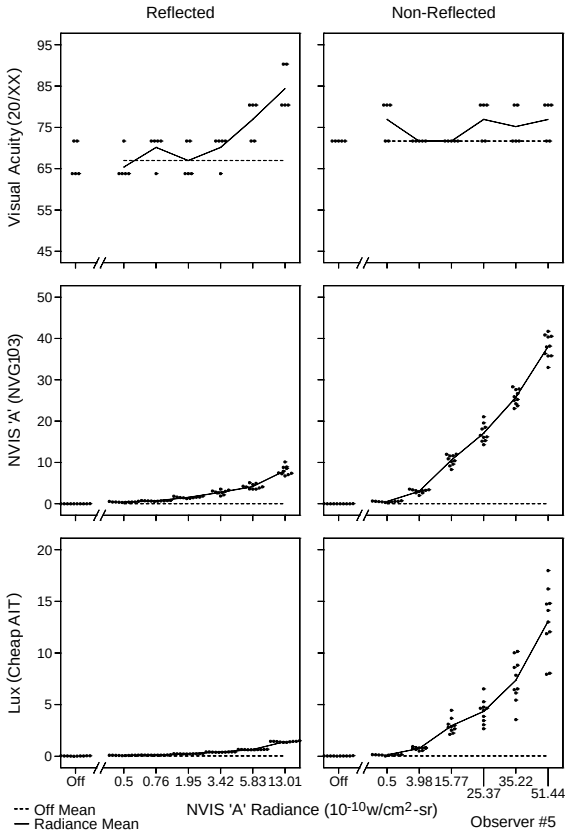

Figure 3. Example of one observer's raw data. Top row is visual acuity data, middle row is NVG 103 data, and bottom row is NVG luminance output data.

This pairing technique produces 25 scores for each NVIS radiance level (five *off* acuities paired with 5 *on* acuities for each radiance). The top row of Figure 4 shows the results of this acceptance/rejection scoring technique for the visual acuity, Task 1.

For the NVG 103 level, the NVIS radiance level of 1.7×10^{-10} watts/cm^2-sr was selected as the acceptance/rejection criteria level. For the NVG luminance output, a value of 0.32 was selected, since that approximately corresponded to the 1.7×10^{-10} watts/cm^2-sr NVIS criteria level determined by empirical measurement.

Figure 4 is a summary of the percent rejection across all 10 observers as a function of the NVIS radiance levels. Note that the radiance levels used for the non-reflected condition were much higher than for the reflected condition, in an attempt to obtain a visual acuity effect in the non-reflected mode.

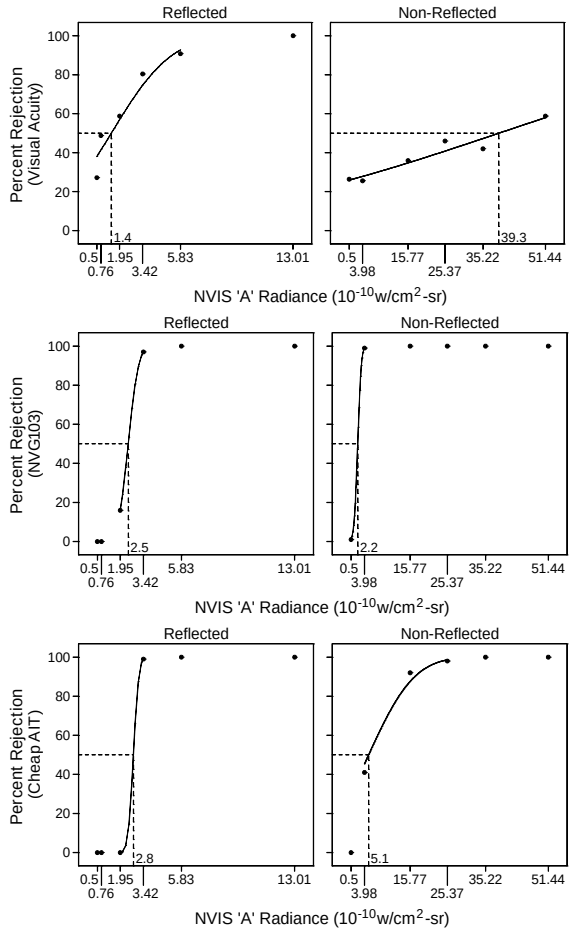

Figure 4. Acceptance/Rejection study results for the two reflection conditions and the three assessment tasks. Vertical axis in each chart is the percentage (or probability) of rejection of the lighting system as incompatible.

Sample sizes for each radiance level were as follows: visual acuity task, n = 250; NVG 103 task, n = 100; NVG luminance output task (labeled as "cheap AIT"), n = 100. Probit analysis was used to fit the percent rejections[9]. The dashed lines indicate the estimated NVIS radiance level that corresponds to a 50% rejection probability.

DISCUSSION

Although the 50% rejection probability NVIS radiance values are noted on the six graphs of Figure 4, these values may not depict the most important aspect of these curves. Ideally, one would like an acceptance/rejection criteria that produces a steep curve cleanly separating the acceptance from the rejection regions. The specific NVIS radiance values used were subjectively set by the experimenter to cover the gamut from no visual acuity interference to

essentially 100% visual acuity interference. It is apparent in the upper left graph of Figure 4, that the visual acuity assessment task resulted in a fairly slowly rising curve, even in the relatively tightly controlled reflected condition. For the non-reflected condition, there is certainly a trend toward higher probability of rejection, as the NVIS radiance increases, but the curve is exceedingly wide, indicating a considerable lack of precision.

Another point should be made regarding the visual acuity curves. It appears that the current rejection criterion of $1.7x10^{-10}$ watts/cm^2-sr is probably not low enough for light sources that reflect in the windscreen but excessively low for light sources that do not reflect in the windscreen.

The middle row of figures illustrates the NVG 103 radiometer data. This device uses an actual image intensifier tube and a brightness matching technique to determine the NVIS radiance. While looking through the device, the user adjusts the brightness of a small internal luminance patch until it matches the brightness of the object of interest. Figure 4 shows that the NVG 103 provides a very sharp rejection criterion when compared to the visual acuity method, even though it is a relatively inaccurate device. It should be noted that this condition was different than the other two. For both the reflected and the non-reflected conditions, the NVG 103 was pointed directly at the light source of the NLS, since the military baseline method ignores the reflection or non-reflection issue.

Figure 4, row 3, illustrates the results of the data collected with the inexpensive illuminance meter (cheap AIT). The concept behind this approach is that the cockpit lighting should add very little light to the output of the NVG image, if the lighting is properly compatible. Since the NVGs, with the attached illuminance meter, were always pointed toward the windscreen of the NLS, the mechanism by which they received light differed between the reflected and the non-reflected conditions. In the reflected condition, the NVGs were amplifying the reflected image of the NLS light source. In the non-reflected condition, some light from the NLS light source could have been imaged directly into the NVGs. This was due to the observer holding the NVGs, such that the NLS light was within the field of view. Nevertheless, the cheap AIT provided a rejection curve that fell between the curve of the visual acuity method and that of the NVG 103.

CONCLUSIONS

Results from the alternate visual acuity assessment study clearly show that NVG cockpit lighting compatibility assessment can be accomplished using inexpensive equipment. It is also evident from Figure 4 that the visual acuity assessment procedure is prone to both Type 1 and Type 2 errors, due to the relatively broad nature of the curve. Furthermore, it is apparent that the NVIS radiance-based criteria, currently used by the military, does not adequately address the difference in visual impact of a reflected light source versus a non-reflected light source.

The NVG 103 provided much better results than the visual acuity assessment, although it does not differentiate between reflected and non-reflected light sources, as noted above.

The NVG light output measurement (cheap AIT) looks very promising as a possible objective method of verifying NVG compatible cockpit lighting. Issues that still need to be addressed, using this device, are calibration procedures and the establishment of a criterion level.

REFERENCES

1. RTCA/DO-275, 12 October 2001. *Minimum operational performance standards for integrated night vision imaging system equipment*, prepared by SC-196, Washington, DC.

2. Task, H. L., & Griffin, L. L. (1982). PAVE LOW III: Interior lighting reconfiguration for night lighting and night vision goggle compatibility. *Aviation, Space & Environmental Medicine, 53*, 1162-1165.

3. ASC/ENFC 96-01 REV 1, 22 March 1996. Interface document, lighting, aircraft, interior, Night Vision Imaging System (NVIS) compatible. Wright-Patterson AFB, OH: ASC ENFC.

4. MIL-STD-3009, 2 February 2001. *Dept of Defense interface standard for lighting, aircraft, Night Vision Imaging System (NVIS) compatible*.

5. MIL-L-85762A, 26 August 1988. *Military specification, lighting, aircraft, Night Vision Imaging System (NVIS) compatible*.

6. Reising, J. D., Antonio, J. C., & Fields, B. (1995). *Procedures for conducting a field evaluation of night vision goggle-compatible cockpit lighting*. (Report No. AL/HR-TR-1995-0167).

7. Reetz III, F. (1987). *Rationale behind the requirements contained in military specs MIL-L-85762 and MIL-L-85762A.* (Technical Report NADC-87060-20). Warminster, PA: Naval Air Development Center.

8. Interagency Agreement DTFA01-02-X-02017 (February 2002) between the Federal Aviation Administration (FAA) and the Department of Defense Air Force Research Laboratory (AFRL/HEC, Wright-Patterson AFB).

9. Finney, D. J. (1980). Probit analysis (3rd ed.). Cambridge: Cambridge University Press.

ACKNOWLEDGEMENTS

The authors gratefully acknowledge the excellent technical support of Sheldon Unger and David Sivert of Sytronics, Inc., Dayton, OH.

A TOOL FOR DETERMINING IMAGE DISCRIMINABILITY

Michael S. Landy†
Department of Psychology & Center for Neural Science
New York University

We describe *discrim*, a Matlab-based program for investigating image discriminability in various display systems. *Discrim* allows the user to manipulate images representing scene content. These images can be built up out of image primitives (sine wave gratings, Gabor patches) and image files from other sources. The user may then manipulate a model of the sensor and display characteristics. The sensor and display model consists of four stages: an initial spatial filter preceding the sensor, Poisson noise, a point nonlinearity ("Gamma") and output noise. The user may view the effects each of these stages has on the image. Finally, the user may specify a pair of images as input to an image discriminability model.

INTRODUCTION

In recent years, a number of computational models have been proposed for early visual coding, leading to models of various visual tasks such as detection, discrimination and classification. In this paper, we describe a program, *discrim*, that was originally written to allow the user to manipulate images and apply image discrimination models to them. It has been substantially revised recently, and now includes the ability to model both the human observer as well as the sensor and display system that is used to detect and display the image materials (e.g., night vision equipment). *Discrim* is fully described in a user's manual. Here, we concentrate on the capabilities of the program as well as some general design issues.

Display system model

Image sensors and display systems have a number of characteristics that can impact the ability of human observers to use the resulting displayed images. This is particularly true in challenging sensor environments such as the low-light conditions that require the use of night-vision equipment. In such conditions, visual displays are photon-limited. To contend with the lack of light, sensor systems must lower spatial resolution (effectively integrating over larger areas of the image), lower temporal resolution (integrating over time) and/or become more quantum efficient. All of these factors have an effect on image quality and hence on human performance using the resulting displays. Image sensors and display systems are typically modeled as a series of image manipulations including spatial filters, point nonlinearities and corruption by noise. *Discrim* implements a simple sensor and display model consisting of four stages. These are, in order of application, (1) a linear spatial filter, (2) Poisson input noise, (3) a point nonlinearity, and (4) Gaussian output noise.

Spatial filter

The input spatial filter may be used to mimic the effects of the optics of the image sensor. *Discrim* can apply several types of filters. One type is a 2-dimensional, Cartesian-separable Gaussian. Very loosely speaking, Cartesian-separable means that the filter may be specified as a product of a filter applied to the horizontal frequencies multiplied by one applied to the vertical frequencies. A second type is a Cartesian-separable filter with the vertical and horizontal modulation transfer functions supplied in a file. Finally, the user can specify a filter that is difference of Gaussians, each of which is Cartesian-separable.

Poisson input noise

The user may specify, or have the program compute, the mean quantum catch of the individual sensor pixels. When that quantum catch is low, as it must be in the low-light conditions for which night vision equipment is designed, the effects of the Poisson statistics of light become important. As an example, Fig. 1

shows a 128×128 image of a sine wave grating with Poisson noise, assuming an average quantum catch of 10 photons per pixel.

Point nonlinearity

The user may specify the nonlinearity applied to individual pixels. Typically, both image sensors (film, vidicons, etc.) and image displays (CRTs, in particular) are characterized by a so-called "gamma curve". *Discrim* includes a single nonlinearity in its sensor and display model. One can think of it as a lumped model that combines both the sensor and display nonlinearities. We implement a minor generalization of the gamma curve by allowing for a level below which no output occurs (which we call "liftoff"). Thus, the output of the nonlinearity is $y = \lfloor x - x_0 \rfloor^{\gamma}$, where x is the input level, x_0 is the liftoff level, and γ is the degree of nonlinearity (2.3-3 is a typical range of values for a CRT system, and such values are often built into devices, such as DLP projectors, which don't have an implicit pixel nonlinearity). Fig. 2 shows an example of the window used in *discrim* to specify the current gamma function.

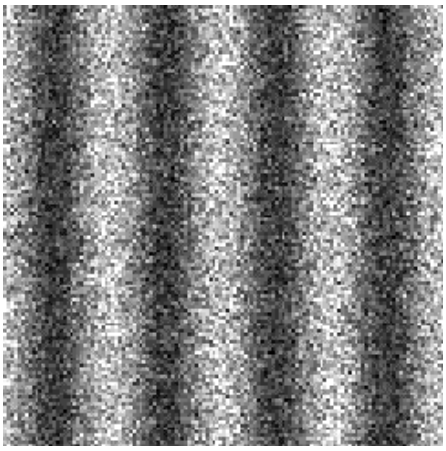

Figure 1. A sine wave grating corrupted by Poisson noise.

Output noise

Finally, *discrim* includes the option of having Gaussian noise added to the displayed pixels after the point nonlinearity has been applied. This may be used to model imperfections in the display device, but can be used for other modeling applications as well (e.g., models of medical imaging devices).

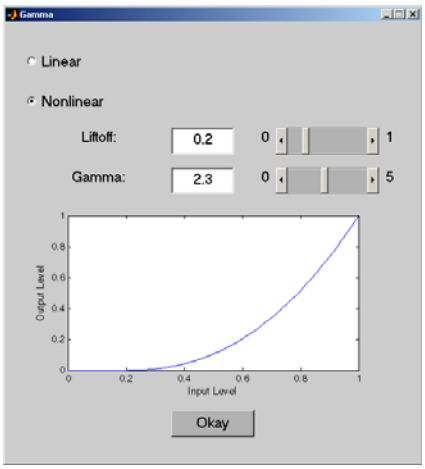

Figure 2. Specification of the gamma curve in *discrim.*

Observer model

In recent years, a number of computational models have been proposed for early visual coding. These models are based on known facts of the early architecture of the human visual system as well as taking into account empirical observations of human performance in visual discrimination tasks.

Several aspects of the visual system are typically reflected in vision models. They may include any or all of the following. (1) *Spatial channels.* Early in the visual system, patterns are coded using channels tuned for spatial frequency and orientation. Typical bandwidth estimates are one octave in spatial frequency and 30º in orientation. Peak sensitivity varies with spatial frequency, and the envelope of channel sensitivities results in the human contrast sensitivity function. (2) *Retinal inhomogeneity and sampling.* The peak sensitivity, range of spatial frequencies coded and density of sampling varies as one proceeds from the fovea to peripheral locations. (3) *Masking.* Target patterns are generally, although not always, more visible on a uniform background than in the presence of other patterned visual input.
By and large, current visual models result in a vector of responses from the modeled channels that serves as the code for the input image. Vision models may be used to predict the results of typical tasks faced by the visual system,

including (1) *detection*: visibility of a pattern against a uniform background; (2) *discrimination*: ability to detect the difference between two images, which includes detection of a target against a non-uniform background; and (3) *classification*: determining whether a pattern, viewed alone or on a noisy background, is one of *n* possible test patterns (e.g., letter identification). At present, *discrim* includes a single image discrimination model called the "single filter, uniform masking" (SFUM) model (Ahumada, 1996; Ahumada & Beard, 1996, 1997a,b; Rohaly, Ahumada & Watson, 1997). The model includes a contrast sensitivity function as well as a simple model of pattern masking. SFUM was designed to estimate the value of d' for discriminating two given, fixed images. For example, in evaluating a lossy image compression scheme, SFUM will provide an estimate of the ability of an observer to discriminate an original image from its compressed, distorted counterpart. The resulting d' (pronounced "d prime") value indicates the degree of discriminability. A d' value of zero indicates the two images are completely indiscriminable, so that an observer would be 50% correct (i.e., guessing) on a two-alternative forced-choice (2AFC) task. d' values of 1 and 2 correspond to performance of 76% and 92% correct in a 2AFC task, respectively.

The *SFUM* model was designed to estimate the discriminability of a pair of fixed images. The display model, described in the previous section, involves two possible sources of noise: input Poisson noise and output Gaussian noise. When either or both of those noise sources are enabled, the intent of the *discrim* program is to allow the user to estimate the discriminability of the two input images under conditions of stochastic variability due to the noise source(s) (and other image distortions). That is, on any given trial an observer will see a different retinal image due to the variability of the noise from trial to trial. If we simply added different, independent Poisson and/or Gaussian noise samples to each of the two images and then applied the SFUM model, SFUM would attempt to estimate discriminability not only of the underlying images, but of the two noise samples as well. Clearly, this is not appropriate. What is of interest is the observer's ability to discriminate the underlying scenes despite the noise, not their ability to discriminate the noise samples.

Thus, the SFUM model is not well-suited to the problem at hand. However, we have implemented the SFUM model in a way that should allow it to provide reasonable estimates. We do this by using the same sample of noise, Poisson and/or Gaussian, for both images. Thus, there are no differences between the two noise samples that artificially inflate the d' estimates. Gaussian noise is an additive process that is independent of the image content. It is a simple matter to generate a Gaussian noise image, and add it to both input images. On the other hand, Poisson noise depends on the image content. The variance of the noise added to any given pixel is equal to the value of that pixel. This means that the use of the same noise image for both input images is not an accurate reflection of Poisson statistics. We have settled on an approximation that we feel is adequate for the sorts of threshold detection tasks for which *discrim* is most appropriate. When Poisson noise is used with the SFUM model, the two input images are first blurred using the current spatial filter. The blurred images are averaged, and that average image is subjected to Poisson noise. The difference between the noisy image and the average image (the *error image*) is treated as an additive noise source. That error image is then added to the individual blurred images to simulate a Poisson noise source that perturbs both images identically. Note that each time *discrim* calculates a d' value, new samples of Poisson and/or Gaussian noise are used. Thus, the user can average over several such calculations to guard against an outlier value due to an atypical noise sample.

The *discrim* program is designed to be able to include additional vision models. In particular, there is a large literature (mostly from the medical imaging community) of visual detection and discrimination models for visual targets in patterned and noisy backgrounds (Barrett, Yao, Rolland & Myers, 1993; Bochud, Abbey & Eckstein, 2000; Burgess, 1999; Burgess, Li & Abbey, 1997; Eckstein et al., 2003; King, de Vries & Soares, 1997; Myers et al., 1985; Rolland & Barrett, 1992; Wagner & Weaver,

1972; for reviews see Eckstein, Abbey & Bochud, 2000; Wagner & Brown, 1985). These models provide an estimate of d' given the input images and descriptions of the noise (variance, spatial correlation, etc.). Thus, for these models, *discrim* is already set up to provide the required information, and the issue of using identical noise samples for the two input images shouldn't arise.

Discrim: a tool for modeling image discriminability

Fig. 3 shows the main window of *discrim*. The program is written in the Matlab language. It provides a number of capabilities in the main window, through menus, and through pop-up subwindows that are invoked via a menu. The user builds up a library of input images that are either read in from files or constructed using various built-in image manipulation primitives. On the main window, two of these images can be displayed (here, two slightly different airport images are shown). The currently active image is distinguished by its magenta outline. A button below the images allows the user to request that *discrim* calculate d' for discriminating the two images currently displayed, using the current parameters that govern the display and observer models.

There are six menus available. The *Model* menu is for choosing the image discriminability model to be simulated. Currently, SFUM is the only available choice.

The *Model Parameters* menu brings up a pop-up window for setting the parameters for each available image discrimination model. Currently, the only choice is to invoke a window for setting the parameters of the SFUM model. These include parameters controlling its contrast sensitivity function and the degree of masking.

The *Image* menu allows the user to create, delete, load and save images. Note, in *discrim* the library of images that are created and manipulated are *input* images. That is, they are the raw, undistorted images describing the scene presented to the display model. These images are undistorted by the display filter, Poisson input noise, gamma curve or output noise.

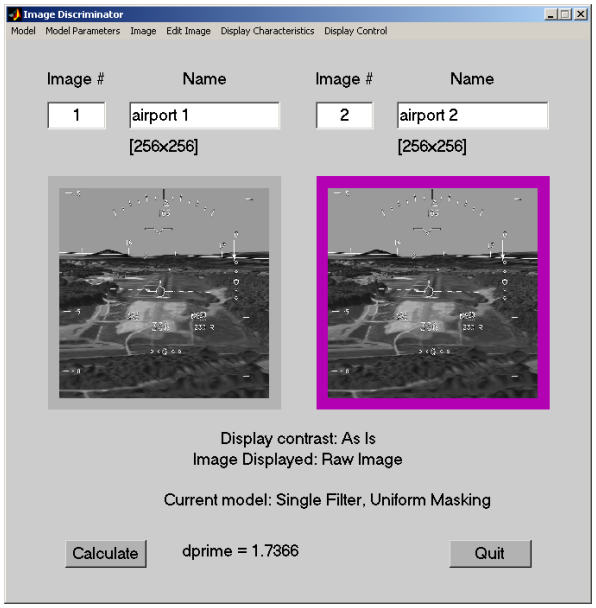

Figure 3. The main window of *discrim*.

The *Edit Image* menu allows the user to manipulate the images. One can add a pattern to an image (sine wave gratings, Gabor patches). Two images can be combined (e.g., adding a target to a background). An image can have its contrast scaled and have extreme pixel values clipped.

The *Display Characteristics* menu is used to control the parameters of the image display model. It is used to invoke pop-up windows for each stage in the display model, including the initial spatial filter, the input Poisson noise, the gamma nonlinearity and the output noise. An additional window allows the user to specify the viewing geometry, including the size of the image in pixels and its visual size.

In Fig. 3, the images shown are input images, undistorted by the various stages of the display model. In the *Display Control* menu, the user can specify which form of image distortion they would like to view.

This includes the undistorted image, as shown, as well as the image after each display distortion has been effected, in turn.

CONCLUSIONS

Discrim is a tool that is easy to use. It is our hope that display modelers and evaluators will be able to use *discrim* to test the quality of displays and their usefulness for particular visual tasks. We are making the code and documentation freely available to the general public at http://www.cns.nyu.edu/~msl/discrim. We hope that others will make use of the software, and will let us know what other capabilities would be useful. Clearly, the most important improvement would be to include additional models of image discrimination, especially those that make allowance for discrimination of noisy images.

REFERENCES

Ahumada, A. J., Jr. (1996). Simplified vision models for image quality assessment. In J. Morreale (Ed.), *SID International Symposium Digest of Technical Papers*, *27*, 397-400. Santa Ana, CA: Society for Information Display.

Ahumada, A. J., Jr. & Beard, B. L. (1996). Object detection in a noisy scene. In B. E. Rogowitz & J. Allebach (Eds.), *Human Vision, Visual Processing, and Digital Display VII*, *2657*, 190-199. Bellingham, WA: SPIE.

Ahumada, A. J., Jr. & Beard, B. L. (1997a). Image discrimination models predict detection in fixed but not random noise. *Journal of the Optical Society of America A*, *14*, 2471-2476.

Ahumada, A. J., Jr. & Beard, B. L. (1997b). Image discrimination models: Detection in fixed and random noise. In B. E. Rogowitz & T. N. Pappas (Eds.), *Human Vision, Visual Processing, and Digital Display VIII*, *3016*, 34-43. Bellingham, WA: SPIE.

Barrett, H. H., Yao, J., Rolland, J.P. & Myers, K. J. (1993). Model observers for assessment of image quality. *Proceedings of the National Academy of Sciences USA*, *90*, 9758- 9765.

Bochud, F. O., Abbey, C. A. & Eckstein, M. P. (2000). Visual signal detection in structured backgrounds III, Calculation of figures of merit for model observers in non-stationary backgrounds. *Journal of the Optical Society of America A*, *17*, 193-205.

Burgess, A. E. (1999). Visual signal detection with two-component noise: low-pass spectrum effect. *Journal of the Optical Society of America A*, *16*, 694-704.

Burgess, A. E., Li, X. & Abbey, C. K. (1997). Visual signal detectability with two noise components: anomalous masking effects. *Journal of the Optical Society of America A*, *14*, 2420-2442.

Eckstein, M. P., Abbey, C. K. & Bochud, F. O. (2000). A practical guide to model observers for visual detection in synthetic and natural noisy images. In J. Beutel, H. L. Kundel & R. L. van Metter (Eds.), *Handbook of Medical Imaging, Vol. 1, Physics and Psychophysics* (pp. 593-628). Bellingham, WA: SPIE Press.

Eckstein, M. P., Bartroff, J. L., Abbey, C. K., Whiting, J. S., Bochud, F. O. (2003). Automated computer evaluation and optimization of image compression of x-ray coronary angiograms for signal known exactly tasks. *Optics Express*, *11*, 460-475. http://www.opticsexpress.org/abstract.cfm?URI=OPEX-11-5-460

King, M. A., de Vries, D. J. & Soares, E. J. (1997). Comparison of the channelized Hotelling and human observers for lesion detection in hepatic SPECT imaging. *Proc. SPIE Image Perc.*, *3036*, 14-20.

Myers, K. J., Barrett, H. H., Borgstrom, M. C., Patton, D. D. & Seeley, G. W. (1985). Effect of noise correlation on detectability of disk signals in medical imaging. *Journal of the Optical Society of America A*, *2*, 1752-1759.

Rohaly, A. M., Ahumada, A. J., Jr. & Watson, A. B. (1997). Object detection in natural backgrounds predicted by discrimination performance and models. *Vision Research*, *37*, 3225-3235.

Rolland, J. P. & Barrett, H. H. (1992). Effect of random inhomogeneity on observer detection performance. *Journal of the Optical Society of America A*, *9*, 649-658.

Wagner, R. F. & Brown, D. G. (1985). Unified SNR analysis of medical imaging systems. *Phys. Med. Biol.*, *30*, 489-518.

Wagner, R. F. & Weaver, K. E. (1972). An assortment of image quality indices for radiographic film-screen combinations – can they be resolved? *Appl. of Opt. Instr. in Medicine, Proc. SPIE*, *35*, 83-94.

† Address correspondence to: Michael S. Landy, Department of Psychology, New York University, 6 Washington Place, Rm. 961, New York, NY 10003, landy@nyu.edu, (212) 998-7857, fax: (212) 995-4349.

FLIGHT TEST PLAN TO ASSESS OF PVFR ROUTES AND SNI OPERATIONS FOR ROTORCRAFT

Stephen M. Hickok and Edwin D. McConkey
Satellite Technology Implementation (STI), LLC, Orange Beach, AL

Background: The concept of Precision Visual Flight Rules (PVFR) and Simultaneous Non-Interfering (SNI) Routes for rotorcraft is based on the hypothesis that rotorcraft with Global Positioning System (GPS) navigation capabilities can stay within narrow, defined horizontal airspace limits while operating under Visual Flight Rules (VFR). If the pilot maintains the aircraft within the confines of a PVFR route and if these routes can be designed to keep rotorcraft separated from fixed-wing traffic then PVFR routes offer rotorcraft the possibility of operating in congested airspace simultaneously with fixed-wing aircraft on a non-interfering basis, hence the term SNI operation.

INTRODUCTION

Many helicopter operators have a requirement to operate using Visual Flight Rules (VFR) in busy terminal areas in a safe and efficient manner in airspace that does not conflict with fixed-wing traffic. Similarly air traffic service providers have a requirement to keep helicopter and fixed-wing traffic separated for safe and efficient terminal area operations. A concept for meeting both requirements is Precision VFR (PVFR) routes, which allow helicopters to operate within defined airspace limits that assure their separation from fixed-wing traffic.

At present there are no standards or flight test data that address issues of the width of PVFR routes or the ability of pilots to follow GPS routes while performing the necessary tasks to operate their aircraft under VFR. While GPS use during VFR operations is common practice in the NAS, the required use of GPS on PVFR routes to keep an aircraft within defined airspace limits has not been validated.

OBJECTIVES

The objective of the PVFR/SNI project is to evaluate the ability of GPS to provide lateral guidance for helicopters flying on PVFR routes while using barometric altitude for vertical guidance. A secondary objective is to develop and demonstrate PVFR routes and ATC procedures that use GPS to enhance the helicopter pilot's ability to navigate more efficiently in the National Airspace System (NAS). The results of this research and development effort will be used by the Federal Aviation Administration (FAA) to determine airspace requirements, air traffic control procedures, and pilot operational and training considerations.

The flight test will assess human factors, flight technical error (FTE), navigation system error (NSE), and total system error (TSE) associated with operating GPS-equipped helicopters during PVFR/SNI operations. FAA can use these assessments to develop policy, criteria and guidance to support implementation of PVFR/SNI operations. Specific operations that may be enhanced by PVFR routes include helicopter transitions through control zones and congested airspace and flights through areas with natural or manmade obstacles, such as mountain passes and valleys.

TEST METHODOLOGY

The FAA has determined that the assessment of PVFR human factors and route widths will be performed by a combination of flight test and simulation methods. This paper describes the flight test portion of the PVFR/SNI project. The PVFR simulation effort is described in another paper prepared by the Naval Postgraduate School (NPS).

A key element of the overall test methodology is to provide means to correlate results of the flight testing and the simulation. This allows simulation to support areas that cannot be adequately addressed by flight testing and vice versa. Agreement between the flight-testing and simulation results offers the opportunity to significantly expand the supporting data.

ROLES AND RESPONSIBILITIES

The flight-test evaluation is the responsibility of Satellite Technology Implementation, LLC (STI) of Orange Beach, AL. STI, under contract to the FAA, is supported by the University of Tennessee Space Institute (UTSI) to provide a test helicopter, maintenance support, safety pilot, and technical assistance.

Overall test coordination and technical direction for the PVFR project is provided by FAA Human Factors Division (AAR-100) located at FAA Headquarters in Washington, DC and FAA General Aviation and Vertical Flight Office (AAR-460) located at the William J. Hughes Technical Center, Atlantic City, NJ. AAR-100 and AAR-460 are supported by the FAA's Flight Technologies and Procedures Division (AFS-400), the sponsoring organization for the project.

TEST PLAN

The conduct of the flight test is governed by the PVFR/SNI Flight Test Plan. The test plan describes all of the elements that comprise the complete test program.

Test Aircraft. STI has selected an Army OH-58A helicopter operated by UTSI to be the test aircraft. A large percentage of helicopter pilots have flown the OH58, its civil variant (the Bell 206 Jet Ranger), or the Navy variant (the TH-57 basic flight trainer). Use of this helicopter addresses a number of test considerations. The test aircraft:

- Is representative of VFR helicopters in widespread use in the NAS,
- Is familiar to most subject pilots,
- Is large enough to carry all necessary test personnel and equipment, and
- Permits the simulation phase of the assessment to model a single helicopter.

The test aircraft is equipped with a Bendix-King Model KLN89B GPS receiver. This is a panel-mounted receiver certified to the standards of FAA's Technical Standard Order (TSO) C129 Class A1.

Subject Pilots. Testing will be completed using 10 subject pilots. Pilots will be a mix of VFR- and IFR-rated pilots with a target of 5 VFR and 5 IFR rated pilots. This mix of pilots is representative of the population of licensed helicopter pilots 'at large'. Some subject pilots will be selected from Navy instructor pilots who will be available to participate in the simulation tests at NPS.

To correlate flight test and simulation results, each subject pilot will wear a head-mounted head and eye tracker during some or all of the test flights. A description of the head and eye tracking system is provided in a separate paper by NASA Ames Research Center.

PVFR Test Route. The flight tests will be performed in the airspace around Tullahoma, TN Regional Airport (THA).

STI designed a route specifically for the PVFR flight testing. This route is representative of VFR routes in use in the NAS and represents a broad range of operational and support conditions, to include:

- Terrain and obstacles are consistent with those found in a VFR route environment,
- Aircraft and test personnel can be supported logistically,
- Test area is suitable for day and night VFR operations,
- Test route represents a realistic ATC environment,
- Route segments and turn angles are representative of a typical VFR route, and
- VFR waypoints[1] are identifiable by terrain or manmade features during day and night operations; waypoints will be connected by straight segments so routes can be defined by overlaying GPS waypoints on the VFR waypoints.

A map of the test area including the PVFR route is shown in Figure 1. The Tullahoma area allows testing of the PVFR/SNI concept in a feature-rich region. Features found along the test route include highways, cell and water

[1] A VFR waypoint is defined as a natural or manmade feature, recognizable to the pilot, which marks the intended path of the aircraft.
A GPS waypoint is defined by latitude and longitude coordinates that can be entered manually or automatically in a GPS receiver.

towers, power lines, bridges, a river, a lake, a dam, a factory complex, and a power plant.

The route is designed to test pilot performance in straight segments and turns. Straight segments range from 1 to 6 NM in length. Numerous turns (20 in all) ranging from 6 to 125 degrees are provided in the PVFR route. For analysis, the turns are divided into 4 conditions. These conditions and the number of conditions per flight are shown in Table 1.

Table 1 Test Conditions - Turn Events per Flight

Condition/ Event	Turn Angle (Degrees)	No. of Turns
1	0-29	6
2	30-59	5
3	60-95	5
4	>95	4

The route segments and waypoints are designed to evaluate several test conditions. Some route segments follow well-defined visual features; some route segments are near (but do not overlie) visual features; and some route segments do not follow any defined visual features. These test conditions will provide indications as to whether subject pilots are relying primarily on GPS or visual navigation cues.

TEST MATRIX

Based on test requirements, STI has constructed a test matrix that supports the objectives of the PVFR/SNI project. This test matrix was used to guide the development of the actual test plan routes.

A total of 14 data collection flights will be flown; 10 flights will be flown during daylight hours; 4 flights will be flown during nighttime hours. Data collection will be performed on all flights. Flights will:

- Originate and terminate at THA with a transition to the PVFR route,
- Be flown during VMC using VFR,
- Be hand flown (no autopilot flights),
- Be flown within the standard cruise speed range for the OH-58A and a speed that is comfortable to the subject pilot (typically 70 to 90 knots), and
- Be conducted using standard rate turns.

Adherence to the test matrix will provide a sufficient number of data sets to assure statistical significance for straight and turning flight.

The test matrix, which relates subject pilots, test conditions, and flights, is shown in Table 2. It provides a familiarization flight to allow each pilot some time to operate the aircraft and systems for approximately 30 minutes prior to the beginning of data collection. Following the familiarization flight the data collection flight will begin.

DATA REQUIREMENTS

Subject Pilot Data. Each subject pilot will complete a pre-test questionnaire and post-flight questionnaires at the conclusion of each flight.

The pre-test questionnaire will provide background information on experience level, currency, aircraft flown, etc. To maintain the privacy of the subject pilots, data on individual pilots will by known only to STI test personnel and will not be released or otherwise made available to the FAA. Pilot data provided to the FAA will be in summary format.

Each subject pilot will complete a post-flight questionnaire to collect the pilot's assessment of the operation of the aircraft and the GPS receiver during the flight. Questions will be of two forms: 1) quantitative ratings to assess the level of difficulty or risk associated with flying or operating the GPS equipment during the flight, and 2) questions soliciting pilot comments on positive and negative aspects of operating aircraft and GPS equipment on PVFR routes. Pilots will be asked to identify specific visual references they used during the flight. This information will be provided to NPS for use in the simulator tests.

True Aircraft Position Digital Data. The true position of the aircraft will be determined by a Time and Space Position System (TSPI). The TSPI consists of a survey quality GPS tracking system. TSPI data is processed post flight to produce highly accurate aircraft true position (less than 1 meter error).

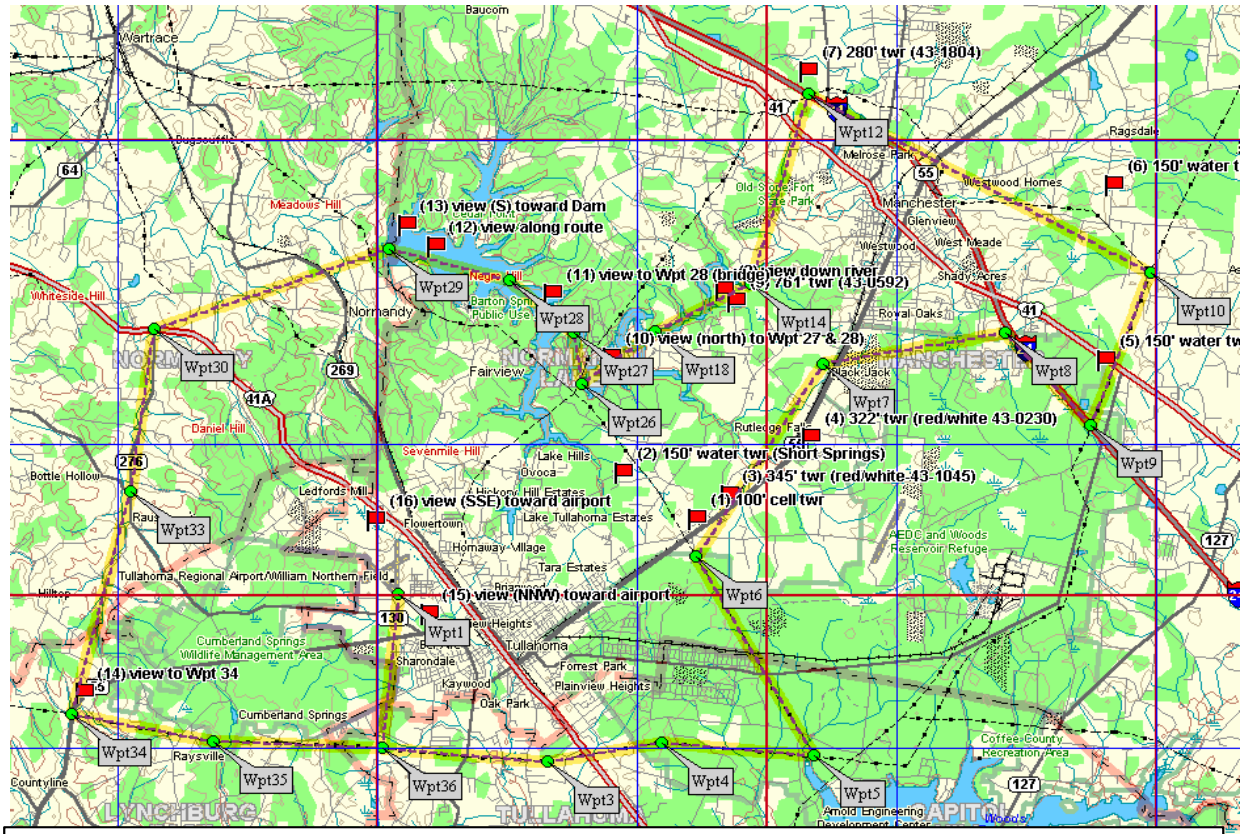

Figure 1 PVFR Test Route (Final Draft)

Table 2 PVFR Flight Test Matrix

Pilot	Rating	Event 1	Event 2	Event 3	Event 4	Total
1	IFR/VFR	6	5	5	4	20
2	VFR-Only	6	5	5	4	20
3	IFR/VFR	6	5	5	4	20
4	VFR-Only	6	5	5	4	20
5	IFR/VFR	6	5	5	4	20
6	VFR-Only	6	5	5	4	20
7	IFR/VFR	6	5	5	4	20
8	VFR-Only	6	5	5	4	20
9	IFR/VFR	6	5	5	4	20
10	VFR-Only	6	5	5	4	20
1	IFR/VFR	6	5	5	4	20
2	VFR-Only	6	5	5	4	20
3	IFR-VFR	6	5	5	4	20
4	VFR-Only	6	5	5	4	20
Data sets	**(minimum)**	**60**	**50**	**50**	**40**	**200**
Data sets	(optional)	24	20	20	16	80
Data sets	(total)	84	70	70	56	280

10 day flights – number and makeup of subject pilots:
(1) 50% IFR/VFR
(2) 50% VFR-Only
(3) Operational pilots from private, industry, and military (Navy).

4 night flights – number and makeup of subject pilots:
(1) Two IFR/VFR pilots form military (Navy)
(2) Two VFR-Only pilots from private industry.

Note: Pilots 1 through 4 fly one night flight and one day flight. Pilots 5 through 10 fly one day flight.

Airborne Digital Data. Digital data from the aircraft's GPS receiver and altimeter system will be recorded during all test flights by a personal computer (PC)-based data collection and recording system. Data will be recorded at the highest rate available from the receiver. Typically, these data are available at a 1-Hertz (Hz) rate.

Concurrent with the recording of the TSPI and airborne systems data, personnel from NASA Ames will be collecting data on the pilots' head and eye position during the test flights. STI personnel will coordinate with NASA Ames personnel to assure that digital data from the airborne GPS system, the TPSI, and the head and eye tracker are time-correlated. This will allow an assessment of FTE error growth during times that the pilot's attention is focused on tasks outside the cockpit.

Flight Log. The onboard flight test engineer will maintain a flight log. The engineer will record details of the flight including: subject pilot number; test run number; start and end flight time; pilot verbal comments; reported temperature and winds; and any other information considered pertinent by the flight test engineer.

Data Reduction. Data from the PC-based onboard digital data recording system will be time-merged with TPSI data. Data processing software, developed by STI, will produce time series of cross track error. The components of cross track error will be broken down into Navigation System Error (NSE), Flight Technical Error (FTE) and Total System Error (TSE).

TEST EXECUTION

Pre-Test Briefing. Subject pilots will be given a local area orientation and a pre-test briefing describing the purpose of the test, the test route, and the test conditions. The subject pilot will also be asked to complete the Pre-Test Questionnaire at this time.

Familiarization Flight. To establish a baseline experience level for all subject pilots, each pilot will fly a familiarization flight with as many flight segments as needed to become familiar with the test routes and aircraft systems. The familiarization flight route will be different than the PVFR test route used for data collection.

Data Collection Flights. After completing the familiarization flight, the subject pilot will fly one or two data collection flights as dictated by the test matrix. Data collection flights will consist of a VFR departure from THA. The flight then will then transition to a PVFR route for the en route segment. The flight will conclude with a VFR transition from the PVFR route to THA.

Post-Test Debriefing. The subject pilot, safety pilot, and flight test engineer will review events and subject pilot comments from the flight log. They will also discuss general comments on the PVFR test program. In particular, the subject pilot will be asked to discuss areas of concern or uncertainty regarding operational use of PVFR routes. To protect the privacy of the subject pilots, these comments will be treated with confidence by the interview team and will not be attributed to specific pilots. Only summary comments will be provided to the FAA and the identity of the subject pilot making such comments will not be released to the FAA.

SCHEDULE

Key schedule milestones are shown below:

- Test Plan Complete: 06-30-03
- Test Readiness Demonstration: 09-30-03
- Data Collection Complete: 10-31-03
- Draft Test Report Complete: 08-31-04
- Final Test Report Complete: 12-31-04

SUPPORTING DOCUMENTATION

Documents and technical direction related to this test include:

1. FAA Aeronautical Information Manual (AIM).
2. FAA Order 7110.65N; Air Traffic Control

PROGRESS ON THE SIMULATOR AND EYE-TRACKER FOR ASSESSMENT OF PVFR ROUTES AND SNI OPERATIONS FOR ROTORCRAFT

[1]Rudolph P. Darken, [1]Joseph A. Sullivan, and [2]Jeffrey Mulligan
[1]Naval Postgraduate School, Monterey, CA, [2]NASA Ames Research Center, Moffet Field, CA

Background: The concept of Precision Visual Flight Rules (PVFR) and Simultaneous Non-Interfering (SNI) Routes for rotorcraft is based on the hypothesis that rotorcraft with Global Positioning System (GPS) navigation capabilities can stay within narrow, defined horizontal airspace limits while operating under Visual Flight Rules (VFR). If the pilot maintains the aircraft within the confines of a PVFR route and if these routes can be designed to keep rotorcraft separated from fixed-wing traffic then PVFR routes offer rotorcraft the possibility of operating in congested airspace simultaneously with fixed-wing aircraft on a non-interfering basis, hence the term SNI operation (Hickok & McConkey, 2003).

INTRODUCTION

The objective of this research program is to investigate Precision VFR (PVFR) routes for Simultaneous Non-Interfering (SNI) operations in the National Air Space (NAS). For a variety of reasons, it is not practical nor is it safe to investigate these routes exclusively using actual in-flight rotorcraft. The research plan calls for a series of steps which will facilitate this investigation.

1. Conduct a human factors investigation of in-flight performance of pilots during a PVFR route (This phase is described in detail in Hickok & McConkey, 2003).
2. Replicate the same task and environment used in the in-flight study using a virtual simulation. Compare human factors data (visual scan patterns, performance, etc.) to determine if the simulation approximates actual flight and is therefore suitable for further investigation.
3. Assuming the simulator satisfies the requirements set out in the first phases of the program, we can then construct new PVFR routes and collect human performance data to determine their feasibility and predicted improvement over current standards.

The role of the Naval Postgraduate School is to construct the simulation environment for experimentation in the later phases of the program. NASA will construct a mobile eye-tracker for use in data collection. It must be suitable for use both in the actual rotorcraft and in the simulator.

This paper will report on progress in both of these parts of the research program.

THE SIMULATOR

The actual simulator consists of both an apparatus and related software and models. Our approach is to construct a simplified simulator that replicates only those aspects of the piloting task that are relevant to this research program. We have been conducting research on rotorcraft navigation and piloting for several years and have completed a cognitive task analysis and several prototype simulators for the overland navigation task (J. Sullivan, Darken, & McLean, 1998; J. A. Sullivan, 1998).

The Apparatus

The hardware apparatus for the SNI simulator consists of an internal environment (cockpit) to include seat, controls, and simulated gauges, and also a display to simulate the external environment.

The selected aircraft for the experiment is the Army OH-58A. The primary data for pilot performance are airborne digital data of actual position and head and eye position during flight. Tracking the position of the aircraft during simulated flight is relatively trivial. However, it is essential that the simulator replicate the

displays and gauges of the OH-58A in order to be able to compare head position and eye gaze data from the airborne portion of the program to the simulator portion. We currently have a placeholder LCD panel for simulated gauges but a plan is in place to replace this with a full scale panel from OH-58A specifications. We will still use LCD panels to drive the gauges but will use a cut-out in the panel with the LCD panel showing where needed.

In Figure 1, we show the apparatus inside the projection screens. The LCD panel will be replaced shortly.

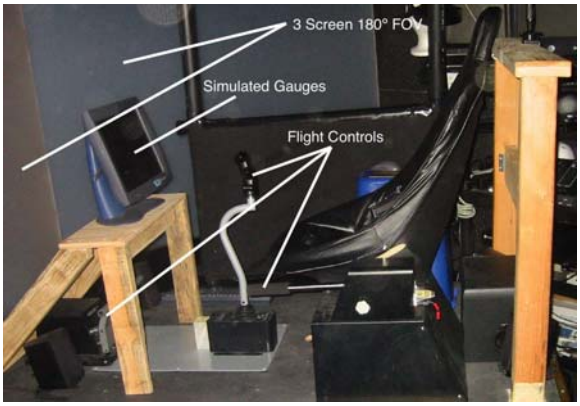

Figure 1. The SNI simulator apparatus.

To simulate the external environment, we use a 3-screen wide field-of-view display. In the virtual environment literature, this is commonly referred to as a CAVE (Cruz-Neira, Sandin, & DeFanti, 1993). Our simulator can also use a Chromakey™ "bluescreen" mixing capability that uses a head-mounted display with a camera mounted on it (Lennerton, 2003). This apparatus is likely unusable for this application, however because of incompatibilities with the eye-tracking device.

In Figure 2, we show a pilot in the simulator during use. The screen behind the pilot is a surrogate for the frame of the aircraft to limit the visual field similarly to the actual airframe.

Figure 2. The SNI simulator during use.

The Virtual Environment

The environment chosen for the experimentation plan is the region immediately surrounding Tullahoma, TN Regional Airport (THA). Satellite Technology Implementation (STI) designed the flight routes as described in Hickok & McConkey (2003). A portion of the flight route is shown in Figure 3.

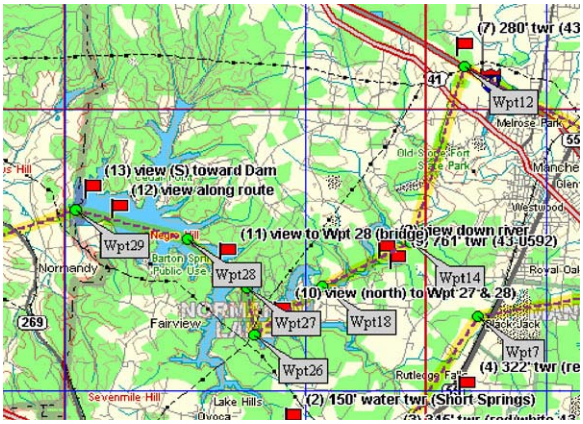

Figure 3. A portion of the flight route (from Hickok & McConkey (2003).

After the region was selected, we collected publicly available digital data of the area and began to construct the virtual model for use in the simulator. We have used Digital Terrain Elevation Data (DTED) and aerial imagery to compose the model shown in Figure 4. We have

approximated the locations of three of the waypoints also identified in Figure 3.

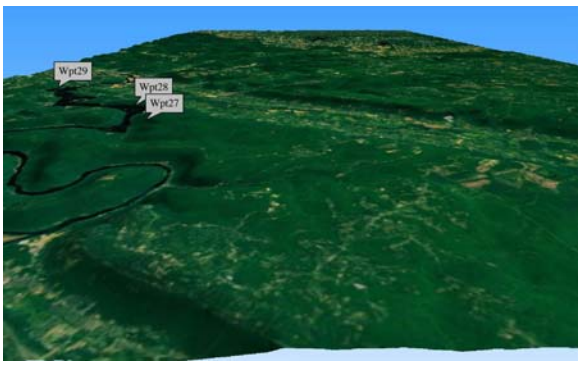

Figure 4. The virtual model.

The model is a work in progress. We have not yet implemented low-level features that will be needed for the PVFR route. The STI team will inform us of these features and their locations. We will then take photographs as needed and place these objects on the virtual model. The model is then imported into the simulation environment so that the virtual helicopter can fly through virtual Tullahoma.

EYE-TRACKING

The objective of the eye tracking portion of the project is to capture head pose and eye gaze position during flight, either simulated or actual. Actual flight is obviously the more difficult of the two due to size and power constraints. The data must be captured and time stamped for later evaluation.

Ames Portable Eye-Tracker

The purpose of this technology development project is to develop a lightweight, comfortable head-mounted eye tracking device suitable for extended use in operational environments. The basic design is patterned on a prototype developed at the Rochester Institute of Technology, and is based on a raquetball eye shield. A portion of the plastic lens is cut away and replaced with an adjustable "hot mirror" which allows the subject a clear straight-ahead view, but reflects an infrared image of the eye to a small camera mounted on the side of the frame. A second forward-looking camera records the "subject's eye" view of the scene, which is used to locate the subject's head within the experimental environment. Images from the cameras are tiled into a single video signal using a "quad processor", and then are recorded for later analysis. The head mount may be directly connected to the recording unit ("tethered" operation), or connected using a 2.4 GHz wireless link. Before recording, time code is added to the signal; the initial time for the time code generator can be derived from a GPS receiver, and GPS position information (sampled once per second) may also be recorded.

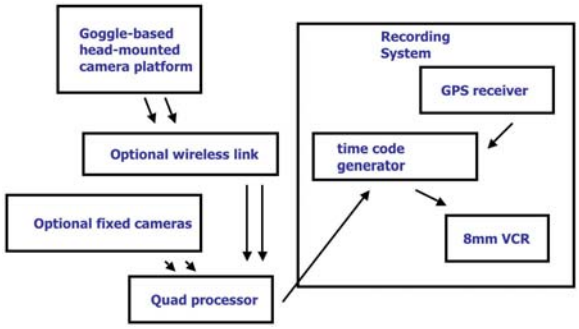

Figure 5. Schematic diagram of the eye-tracking device.

Head Pose Estimation

While the head-mounted camera unit described above has the highest potential gaze-tracking accuracy, there may be situations in which it is impossible to use a head mount. Therefore, we are also exploring technologies to recover gaze using images from a remote, fixed camera. In such images, the subject's eye may only subtend a few pixels, and in this case there is insufficient data to determine eye gaze. However, in normal behavior, the eye rarely deviates more than 5 or 10 degrees from primary position (straight ahead in the head), and so the pose (orientation) of the head can be used to obtain a crude estimate of gaze.

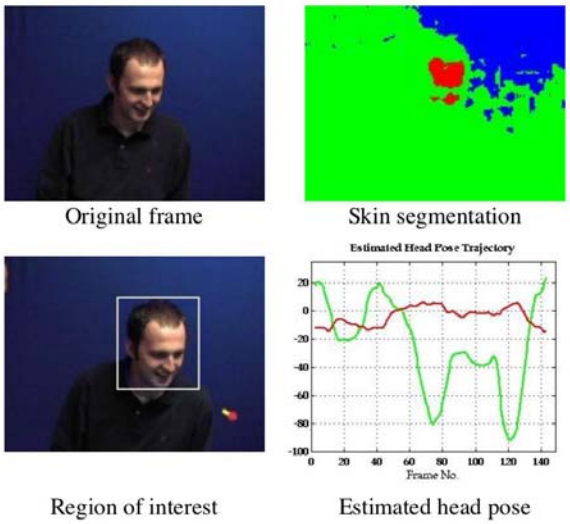

Figure 6. Head pose estimation.

The problem of head-based gaze tracking can be divided into a few distinct components:

1. We must find the head in the image
2. Once we have located the head we must estimate the pose.

When color is available, it is often possible to easily find the face using a color based segmentation (see Figure 6). For monochrome images we have also explored a template-matching algorithm. To estimate the pose parameters, we have investigated methods for directly mapping the image to parameter values. To do this, we start with a training set of images with known pose values; a principal components analysis is then used to extract the "eigenfaces", a set of images which captures the variation between the images in the training set. By restricting analysis to the first few eigenfaces, a large reduction in dimensionality is achieved. Finally, we solve for a polynomial function of the eigenface coefficients that comes closest to predicting the pose parameters in the training set. We have achieved accuracy of a degree or two using a synthetic training set. Current work is in progress to develop a training set based on real images, where the pose parameters used for training are taken from a 3-D model of the test subject's head.

This is not the primary approach we envision for the SNI program at UTSI but it is a suitable technology that may be useful either in the aircraft or the simulator. We will know if this is needed after preliminary testing concludes shortly.

Head-Based Gaze Tracking

Once we have determined the gaze direction (be it of the eye or head), we still need to determine the location or object in the environment that is the target of gaze. To do this automatically, it is necessary to develop a model of the environment. Figure 7 shows an example taken from the interior of a control tower simulator, but the principles are the same for a cockpit or any other environment. We begin by constructing a model of the environment; in this case we used architectural drawings and on-site measurements to construct the model. Next, we determine the position of the virtual camera for which the rendered model is aligned with the video data. Once that has been accomplished, we grab the image texture from the video and "paste" it onto the surfaces of the model. We can then re-render the model from novel viewpoints, including the "subject's eye" view. After the position of the subject's head has been determined, the estimated head pose can be used to cast a gaze vector; the intersection of this gaze vector with a model surface yields the point of regard in the scene.

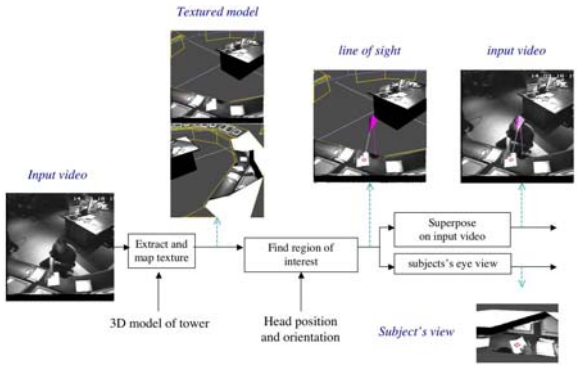

Figure 7. Head-based gaze tracking

The procedures for automatic determination of the camera position will also be used for video based head-tracking with the portable eye-tracker.

The first prototype device for the experiment has been designed and is currently undergoing testing at NASA Ames. On July 2nd the first outdoor test was made, and the need for some additional optical baffling was discovered. Construction of the second goggle is nearly complete. A different battery has been selected for the power source and the power supply regulator issues have been solved. Most of the remaining outstanding issues will not be clearly defined until the July integration trip to UTSI.

SCHEDULE

Key schedule milestones are shown below:

- Test Readiness Demonstration: 09-30-03
- Data Collection Complete: 10-31-03
- Simulator Complete: 12-31-03
- Simulator Test Plan Draft: 03-01-04

REFERENCES

Cruz-Neira, C., Sandin, D., & DeFanti, T. (1993). Surround-Screen Projection-Based Virtual Reality: The Design and Implementation of the CAVE. *Computer Graphics*, 135-142.

Hickok, S.M. and McConkey, E.D. (2003) Flight Test Plan to Assess PVFR Routes and SNI Operations for Rotorcraft

Lennerton, M. (2003). *Exploring a Chromakeyed Augmented Virtual Environment as an Embedded Training System for Military Helicopters.* Unpublished Masters, Naval Postgraduate School, Monterey, CA.

Sullivan, J., Darken, R., & McLean, T. (1998, June 2-3, 1998). *Terrain Navigation Training for Helicopter Pilots Using a Virtual Environment.* Paper presented at the Third Annual Symposium on Situational Awareness in the Tactical Air Environment, Piney Point, MD.

Sullivan, J. A. (1998). *Helicopter Terrain Navigation Training Using a Wide Field of View Desktop Virtual Environment.* Unpublished Masters thesis, Naval Postgraduate School, Monterey, CA.

SUPPORTING DOCUMENTATION

Documents and technical direction related to this test include:

1. FAA Aeronautical Information Manual (AIM).
2. FAA Order 7110.65N; Air Traffic Control

Appendix II

Human Factors Vertical Flight

Research Requirements

Below are the requirements that pertain to the projects listed in Appendix I.

Research Requirement

NVG lighting requirement

NVG resolution requirement

Simultaneous Non-interfering Operations - Quantify VFR Navigation Performance

Requirement ID: 799

Sponsor Organization: ASW POC: Lorry Faber

Requirement Title: NVG lighting requirement

Funded Requirement:

- FY02: Yes
- FY03: Yes
- FY04:
- FY05:

Requirement Statement: This research will validate and expand the draft AC material in Part 27 and Part 29 concerning NVG certification for rotorcraft civil operations. This material only suggests one means of compliance which many operators have complained is not cost effective and not the sole means. However, without this research there is uncertainty if another means may be safe to an overall NVG operation. This research is using the aid of the US military since they too have agreed that alternate methods needs to be explored for cost and immediate implementation. Three NVG civil certifications already exist for a FAR Part 27/29 rotorcraft flying under FAR Part 135 operations, with more to follow. The last certification effort had requested an unknown method to both the FAA and DoD. Research and potentially flight testing is required immediately so the appropriate alternate methods can be justified when requested.910

Background: RTCA SC-196 Minimum Operational Performance Standards states a method of compliance for NVG lighting that is very similar to the method employed by the military. Many civilian operators, FAA test pilots and small manufacturers are concerned that this method is expensive and not necessarily the only method out there. However, due to lack of data, the current method is the only one proven to be safely employed as an effective evaluation process. The Committee agreed that this method will be cited in the document with a caveat that this is a recommendation only and that applicants applying for NVG certification has the right to not use this method if another method is appropriately documented and justified. As a result, many FAA and DoD are concerned that the alternate means of compliance that are suggested from applicants may not be totally proven to be safe. Most applicants (or small manufacturers) have limited budgets and therefore do not commit testing funds to R&D as other agencies might do. It is very difficult for the FAA to refute the data if the data is well justified for the small operation. Thus, the impetus for the need for this research.

Output: Final report detailing results of repeatability testing for military accepted methodology and describing the alternative, inexpensive methodologies that provide the same results

Regulatory Link: RTCA-196

Requirement ID: 798

Sponsor Organization: ASW POC: Lorry Faber

Requirement Title: NVG resolution requirement

Funded Requirement:

- FY02: Yes
- FY03: Yes
- FY04:
- FY05:

Requirement Statement: This research will validate and expand the draft AC material in Part 27 and Part 29 concerning NVG certification for rotorcraft civil operations as well as the draft TSO concerning Night Vision Goggles. This material only suggests a minimum NVG resolution requirement that many European manufacturers and US civil operators are too stringent. The requirement was written because no data exists as to the existing acceptable resolution for human being for safe NVG flight. The requirement was a consensus decision based on NVG manufacturer statistics of current product use which did not include a wide variety of resolution levels. However, without this research there is uncertainty if another means may be safe to an overall NVG operation. This research is using the aid of the US military since they too have agreed that alternate methods needs to be explored for cost and immediate implementation. Three NVG civil certifications already exist for a FAR Part 27/29 rotorcraft flying under FAR Part 135 operations, with more to follow. Research and potentially flight testing is required immediately so the appropriate alternate resolutions for NVGs can be justified when requested. This need stems from recent approval for specific civilian use of NVG and the recent completion of the RTCA SC-196 Minimum Operational Performance Standards. Examination of use in expected civilian operations as compared with military operational data to determine specific problems that may be associated with device use (CAMI proposed this examination originally in 1995). This research will contribute to formulating an AC and Noticed for Proposed Rulemaking (NPRM) for civil operations for general aviation and rotorcraft for NVG certification and operations. Also, a Technical Standard Order is needed for the Night Vision Goggle equipment. There is currently no guidance for NVG's except for military specifications and regulations which may not be adequate for civil use. Three NVG civil certifications already exist for a FAR Part 27/29 rotorcraft flying under FAR Part 135 operations. There are other supplemental type certificate applications concerning NVG usage as well as waivers to the operating rules. Research and potentially flight testing is required immediately so the appropriate regulatory statements are written and adopted. 2347

Background: For the past twenty years, the United States military has enhanced situational awareness during night missions by employing night vision devices

(NVD) of various types. These devices enable the user to identify objects in the NVD field of view that are otherwise unrecognizable in the low illumination of the night environment. NVD's have been championed as the tools that virtually turn night into day. Some common employment of NVD's are NVGs by infantry, aviation and naval forces, starlight scopes by infantry, forward looking infrared by aviation and thermal sights by armor units. A specific NVG, Gen III image intensifier tube, amplifies small amounts of light between the spectral range of 600nm to 930nm. The NVG's signal to noise ratio is excellent during high illumination but falls off dramatically during low light conditions. Unfortunately, the majority of military night missions occur below starlight illumination conditions. Consequently, NVG users report decreased visual acuity, poor contrast, increased scintillations, and the loss of depth perception due to degraded texture gradients. As a result, NVG users have a higher probability of making sensory-perceptual errors which are the most common causal factor related to mishaps involving NVG use. In fact, from 1973-1993 US Navy and Marine Corps forces have had 13 rotary wing and 5 fixed wing class A mishaps employing NVGs, resulting in 15 helos, 6 jets, and 39 lives lost. For most NVGs the best visual acuity under ideal conditions is 20/40 resolution. Military pilots corrected or uncorrected visual acuity is 20/20, while Federal Aviation Regulations (FARs) state that civilian nighttime visual acuity must be 20/40. In the military, night vision goggle usage is strictly controlled. The military aviator must maintain physical, training, and performance requirements to use NVGs; however these strict guidelines will be difficult to enforce for civilian NVG users. RTCA 196 Minimum Operational Performance Standards document outlines numerous issues that the Federal Aviation Administration must consider if civilian pilots are authorized to use NVGs. A high priority issue identified by the RTCA 196 committee was NVG resolution – what are the effects of degraded visual acuity on NVG detectability ("Minimum visual acuity (VA) requirements" and "Pilot vision requirements for NVG operations" from Simpson, Turpin, and Gardner, 2001, report entitled "Human Factors Issues for Civil Aviation use of Night Vision Goggles")?

Output: Final report. 1) Incorporate NVG tube MTF values into the MATLAB Image Discrimination model 2) Modify MATLAB graphical user interface to include NVG MTFs and other relevant NVG parameters that may be modeled. 3) Perform NVG detectability analyses for different observers' visual acuities, e.g, 20/10, 20/20, 20/40, 20/60, 20/80, …, 20/200, across the three different NVG tubes (40, 50, and 64 lp/mm).

Regulatory Link: RTCA-196

Requirement ID: 865

Sponsor Organization: AFS POC: Hooper Harris

Requirement Title: Simultaneous Non-interfering Operations - Quantify VFR Navigation Performance

Funded Requirement:

- FY02: Yes
- FY03: Yes
- FY04: Yes
- FY05: Yes

Requirement Statement: To determine NAV performance of VFR helo pilots using IFR qualified GPS receivers. AFS needs to quantify helo pilot NAV performance for IFR and VFR pilotage which will allow the development of procedures to integrate within the national airspace system.255

Background: A major part of the future changes in the NAS to improve operations for helicopters will be the emergence of simultaneous Non-Interfering Operations (SNI) for VFR helicopters and fixed wing traffic (IFR and VFR). To achieve this Airspace Redesign, to what extent is the minimum amount of airspace needed to protect the VFR helicopter flying a SNI leg/route from a human performance standpoint. The proposed concept to be employed is based on satellite navigation technology. In turn, the amount of airspace that would be needed to protect the minimally equipped helicopter will be based on technology. Human Factors questions include: To evaluate the relationship between pilotage and radio navigation. a) what are the ATC procedures that a helo VFR pilot should follow to optimize national airspace capacity? b) what is the amount of time the pilot fixates on landmarks versus GPS output. c) does the pilot fly the GPS needle? During VFR the pilot should use landmark references but the pilot may shift visual attention to the GPS which may adversely affect pilotage. c) does the GPS affect pilot scan?

Output: A report that recommends the minimum Required Navigation Performance (RNP) value for a VFR helicopter equipped with an IFR GPS. The minimum RNP value will help ATC develop procedures for VFR SNI routes

Regulatory Link: This research request is directly linked to HR 1000 Section 103 of the Agency's performance plan. (Implementation of the infrastructure for helicopters and tiltrotors) and Administrator's 2001 Vertical Flight Policy Statement